Polymeric waveguide prism-based electro-optic beam deflector

Lin Sun, MEMBER SPIE
Jin-ha Kim
Chiou-hung Jang
Dechang An
Xuejun Lu
Qingjun Zhou
John M. Taboada, MEMBER SPIE
Ray T. Chen, FELLOW SPIE
The University of Texas at Austin
Microelectronics Research Center
Austin, Texas 78758
E-mail: raychen@uts.cc.utexas.edu

Jeffery J. Maki, MEMBER SPIE
Suning Tang*
Radiant Photonics, Inc.
1908 Kramer Lane, Suite A
Austin, Texas 78758

Hua Zhang
William H. Steier
University of Southern California
Department of Electrical Engineering
Los Angeles, California 90089

Cheng Zhang, MEMBER SPIE
Larry R. Dalton
University of Southern California
Department of Chemistry
Los Angeles, California 90089

Abstract. Beam steering devices without moving parts are highly desirable for their potential application in emerging optical technologies such as holographic optical storage systems, all optical networks, and optical switches. We demonstrate a thin-film waveguide beam deflector device that consists of an electro-optic prism array within a polymer waveguide. An electrode structure defines the prism array within the planar waveguide. The deflection efficiency of 28 mrad/kV and the maximum deflection angle of ± 8.4 mrad at ± 300 V are obtained for this demonstration device. Further optimization of electrode-field poling and processing is likely to improve these results by at least an order of magnitude. © 2001 Society of Photo-Optical Instrumentation Engineers. [DOI: 10.1117/1.1385164]

1 Introduction

Non mechanical beam steering devices are needed in a wide variety of commercial and military applications, including advanced laser radar (ladar), fiber-optic switching networks, photonic phase array antennas, optical sensors, and laser printers. In particular, thin-film electro-optic beam deflectors have the potential for creating a new class of integrated fiber-optic switches in addition to free-space laser beam steering.[1–4] The resulting fiber-optic switch can actively and selectively route a large number of fiber channels using only one electrode, which provides significant advantages over existing devices. These advantages include a simplified operating scheme, low driving voltages, high switching speed, small size, and low cost.

Electro-optic (EO) devices, based on both inorganic crystals and polymer materials, have been investigated widely due to their potential applications in optical communications.[5–7] Beam deflectors based on the EO effect offer the most promising technology for high-speed steering of laser beams without a moving mechanical assembly. Most of the commercially available EO devices are made from inorganic materials such as lithium niobate. They are generally large and heavy, and require relatively high driving voltages ranging over a few kV. Compared to their inorganic counterparts, polymeric materials have the well-recognized advantages of compatibility with different substrates, ease of fabrication, and low cost. Consequently, a large number of EO polymers have been synthesized in recent years.[5–8] However, lack of thermal stability of EO effect in polymeric materials and relatively large insertion losses have raised significant hurdles in the development of polymeric EO devices. We report a thin-film guided-wave EO beam deflector based on a low-loss polymeric material with a large and stable EO coefficient. The fabricated waveguide beam deflector uses a CLD-5 thin film as a core layer and polymeric thin films of Epoxy-9653, and NOA61 as bottom and top cladding, respectively. Compared to our previous work,[9] the improved core material provides a larger beam deflection due to the large EO effect resulting in enhanced index changes in the core with respect to applied electric field variations.

2 Device Concept

The EO beam deflector described here is based on the fact that the propagation direction of the light beam can be

---

*Current affiliation: Digilens, Inc., Sunnyvale, CA 95054.
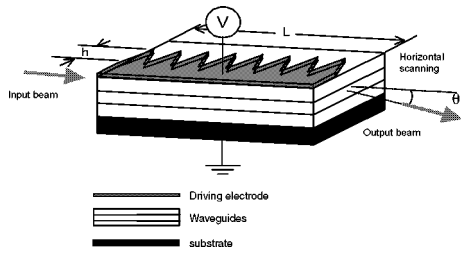
Fig. 1 Schematic diagram of the polymeric waveguide electro-optic beam deflector.

changed by inducing an index pattern in the EO medium by applying an electric field. Figure 1 illustrates the working principle of an EO prism-based beam deflector. The triangular structure of the top electrode induces a triangular variation of index in the core layer made of EO polymeric material. Light propagating through the deflector deviates from its original path at the interfaces between adjacent regions, because of the difference $(n-n_0)$ in the indices of refraction. The index of refraction of the core material in the absence of the field is n_0; when an electric field is applied, the index of refraction under the prism is n. A light beam propagating within the planar waveguide formed by the polymer layers will thus have its direction of propagation modified in a manner similar to that of a beam passing through a set of physical prisms.

As shown in Fig. 1, the device has a multilayer structure. The first layer deposited on a silicon wafer substrate is a metal film (usually gold), which serves as the bottom electrode. The second and fourth layers are low index thin polymeric films that perform as optical-waveguide cladding. The third layer forms the optical waveguide core and has the specific attribute of possessing the EO effect when poled. The fifth layer is a gold layer patterned as a series of identical triangles with bases interconnected for electrical continuity with each other, which forms the top electrode, as further illustrated in Fig. 2. The fabrication and poling processes are described in Sec. 4. The patterned top electrodes induce a bulk second-order nonlinear optical response in the waveguide core of the poled polymer.

For a TM optical mode of the planar waveguide, where the direction of the ferroelectric domain is along the electric field direction as in our device, the change in the index of refraction is given by

$$\Delta n(E) = \frac{1}{2}n_0^3 r_{33}E = \frac{1}{2}n_0^3 r_{33}\frac{V}{d}, \qquad (1)$$
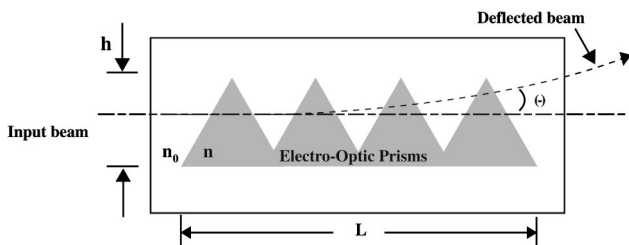
Fig. 2 Schematic top view of the device.
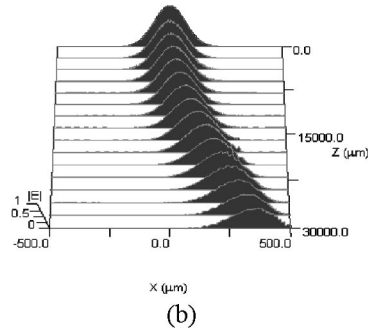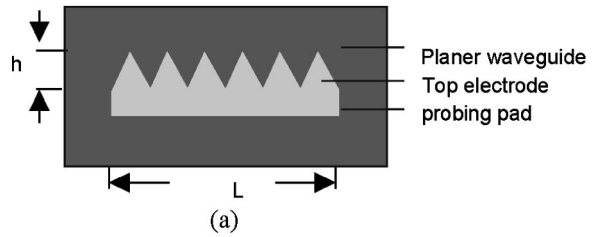
Fig. 3 Schematic of the (a) top view and (b) image of the simulation. We use $L=16$ mm and $h=0.2$ mm.

where r_{33} is the EO coefficient of poled core polymer and V is the voltage applied across the multilayer polymer of overall thickness d. The device produces a deflection angle[10]

$$\theta = n_0^3 r_{33}\frac{V}{d}\frac{L}{h}, \qquad (2)$$

where L and h are the length and width of the prism or the array of prisms, respectively. This model is based only on the total phase retardation possible across the wavefront. The deflection angle in this model depends only on the overall dimension of the prisms, since the accumulated phase difference across the wavefront is independent of how the deflector is subdivided into individual prisms, as long as the interfaces between adjacent prisms are straight lines.

3 Simulation

We have used both ray tracing and a two-dimensional beam propagation method to simulate accurately the operation of the EO deflector. The ray tracing method is the most direct way to evaluate the effect of refraction at each interface. The beam propagation method, however, provides the best information about wavefront quality as well as deflection.

This deflector is simulated with BeamPROP from Rsoft, Inc. This software allows for quick simulation of the device with considerations for electrode placement and the changes it induces in the device via the EO effect. The device that is simulated is a prism array with each prism 0.2 mm at the base, a height of 9 μm, and overall length of 16 mm. The wavelength used for the simulation is 1.3 μm. The core was first thought to have an index of 1.6. It was later measured to have an index of 1.62. The first simulations were done with an index of 1.6. The index of both the top and bottom cladding was set to 1.54. A schematic of the simulated structure is shown in Fig. 3(a). The output beam
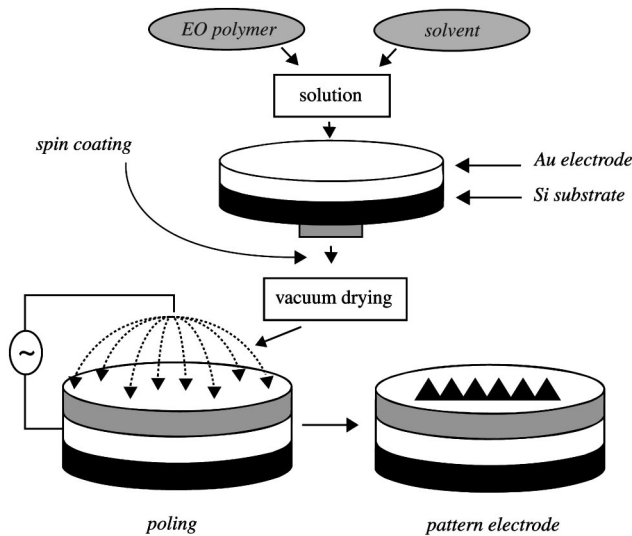
Fig. 4 Flow chart of the process.

Fig. 6 The absorption of CLD-5. The wavelength is in nanometers.

profile was taken on a plane parallel to the input plane with the deflector centered with respect to input and output planes. Figure 3(b) is a typical image of the beam propagating through the deflector. The beam profiles at any point are obtained by taking cross sections of this image at the desired points along the axis of the device. Note that the vertical and horizontal scales are different in Fig. 3(b).

4 Fabrication

The flowchart of the fabrication process is shown in Fig. 4. For an active deflector, the first step is to e-beam evaporate a metal layer, such as gold, onto the silicon wafer. The gold layer acts as a bottom electrode of the device. The electrode consists of 150 Å of chromium followed by 1000 Å of gold. The chromium is used as an adhesion layer for the gold onto the silicon wafer. The planar waveguides are fabricated on gold-coated silicon substrates by spin coating. The waveguide core material is a crosslinkable polymer system consisting of a polyurethane backbone with CLD-5 side chains[11] that have the chemical structure shown in Fig. 5. To achieve high thermal stability, CLD-5 uses a multi-linker to get more rigid crosslinking. It can be readily poled and cured through the simultaneous application of a poling voltage and heat. A corona poling setup with a tip-to-plane distance of 2 cm was used to pole the films. After being precured at 120°C for 1 min and poled at 110°C for 60 min
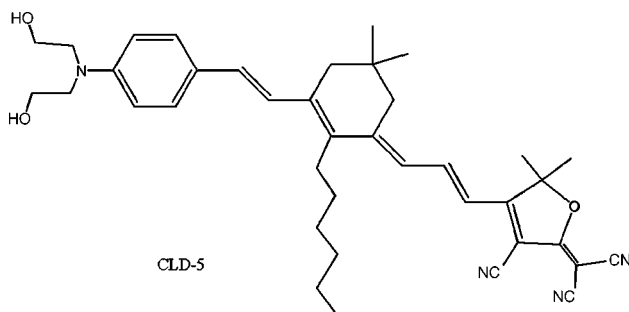
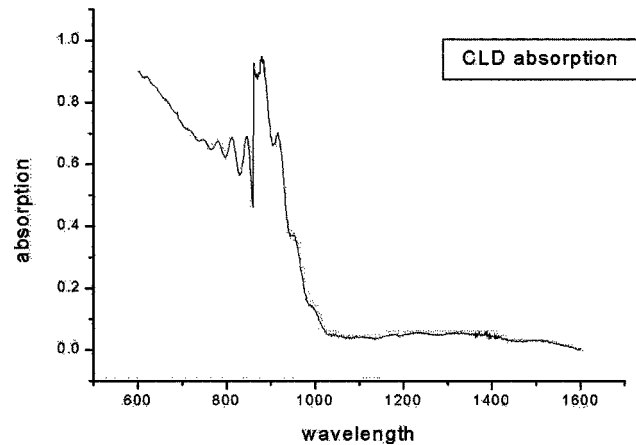with a step-wise voltage profile, the material thereby becomes a fully crosslinked polymer matrix. When the device returns to a nominal temperature and the poling electric field is removed, the poling-induced orientation of the EO chromophores is essentially locked in place because of the complete crosslinking.

The bottom cladding material (Epoxylite 9653-2) has an index of 1.54 at 1300 nm. The core material CLD-5 has an edge at 1010 nm as shown in Fig. 6, such that there is only a small and acceptable absorption at 1300 and 1500 nm. It has an index of 1.62 at 1300 nm. Norland Optical Adhesive 61 (NOA-61), a UV-curable resin with refractive index of 1.54 at 1300 nm, was deposited by spin coating to form the top cladding. A second gold electrode was fabricated on top of this three-layer polymer structure. The top electrode is patterned by wet etching. This top electrode consists of a cascade of prism-shaped regions of thin-film gold. Each prism is connected at its base to the next prism. The design includes a contact pad for easy application of the driving voltage. Each prism has a height $h = 200 \mu$m. The cascade has a length $L = 16$ mm. The device has a length to height ratio $L/h = 80$. Of course, there are many choices for the value of L and h that increase the value of L/h. Clearly, though, the height h of the prisms, which is the width of the active region of the device, should be as small as possible to increase the deflection sensitivity with voltage: but it should also be large enough to contain the laser beam profile.

Figure 7 shows a photograph of the polished end face of one of the planar waveguides. The thickness of the core material is 1.9 μm and the thickness of the top and bottom
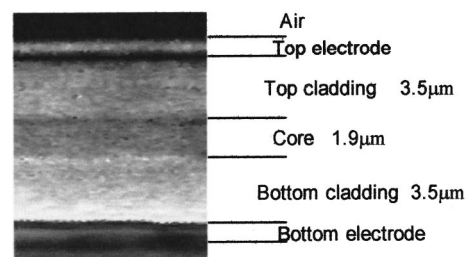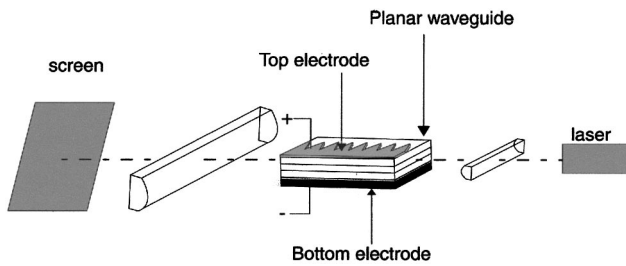

Fig. 5 The chemical structure of CLD-5.

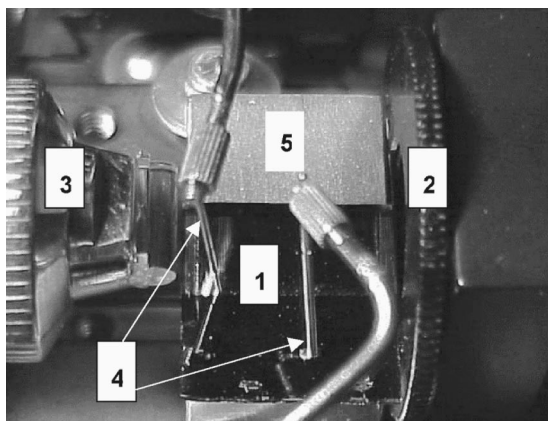**Fig. 7** Microscope photograph of the waveguide cross-section.

Fig. 8 Schematic of the beam-deflector test bed. The screen for observing the beam deflection is placed 32.5 cm from the center of the planar waveguide sample. Cylindrical lenses couple the laser beam into and out of the planar waveguide, respectively.

Fig. 10 Deflection angle plotted as a function of applied voltage.

cladding layers are each 3.5 μm. The edges of the device at each end of the prism cascade are polished to allow light to be coupled efficiently into and then out of the polymer planar waveguide.
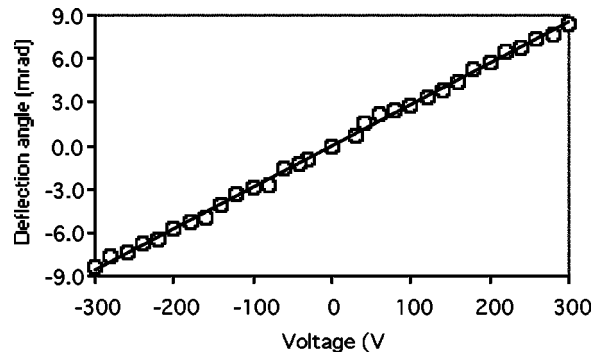
5 Free-Space Beam Deflection

To demonstrate the beam deflection, the planar waveguide sample is mounted on a precision XYZ-stage. The laser light from a diode-pumped Nd:YVO$_4$ laser operating at 1310 nm is end-coupled into the waveguide using a microcylindrical lens ($f = 100 \mu$m). The horizontal spot size at the input end is measured to be 44 μm by the knife edge scanning method prior to placing the device in position. The output beam from the device is refocused using an output cylindrical lens ($f = 2.1$ mm). Figure 8 shows the illustration of the test bed. An opaque white-board screen was placed at a distance of 32.5 cm from the center of the prism cascade of the beam deflector. The transmitted laser beam is incident on the screen. An IR video camera is used to observe the output spot on the screen. The video camera outputs are recorded as still images by a frame grabber and stored as digital images. The magnitude of deflection was obtained by analyzing these images employing a built-in software program. Shown in Fig. 9 is the picture of the test setup.

The measured beam deflection angle versus applied voltage is plotted in Fig. 10. DC voltage ranging from -300 to
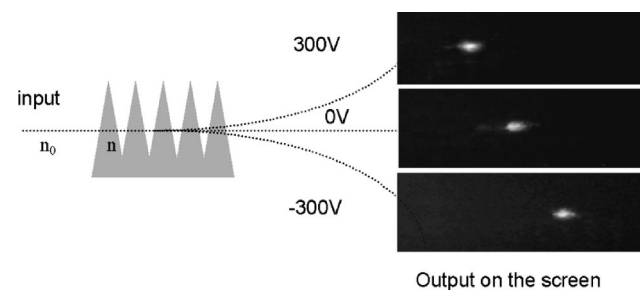
+300 V was applied to the device. The deflection angle shows good linearity with respect to the applied voltage and corresponds to a deflection sensitivity of 28 mrad/kV. Though not quite as sensitive as expected, it is a fairly good performance compared to other EO deflectors previously reported.[12,13] The r_{33} value estimated from Eq. (1) and Eq. (2) is 1.5 pm/V, which is much less than the typical value 27 pm/V. There are several possible reasons for this small r_{33} value. First, the poling strength is not uniform as assumed in the calculations, and the active part of the device may not be in the strongly poled region. Second, pinhole defects in the core film, resulting from the solubility limit of the polymer induced by interchromophore hydrogen bonding, may significantly influence the poling effect. Third, the shape of the index-modulated area may deviate from the shape of the electrode. The fringing in the field pattern should be taken into account to get the precise r_{33} value. Also, the r_{33} value might have decayed due to the relaxation of the oriented dipoles. Even so, this result does not undercut the practicality of EO polymer deflectors.

Figure 11 shows the images of the deflected spots for the applied voltages of ± 300 and 0 V. To show the movement, the photographs are taken one by one. For each voltage setting, we observe some minor changes in the intensity profiles, which are not clearly evident in Fig. 11. The number of resolvable spots, defined by $M = \theta_{\text{def}}/\theta_{\text{div}}$, where θ_{def} is the maximum deflection angle and θ_{div} is the beam divergence angle,[10] is an important parameter to determine the suitability of a deflector. The M value for the demonstrated device is approximately 0.89. This means that there are nearly two resolvable spots within the deflection range

Fig. 9 Testing setup: 1. device under test, 2. input microcylindrical lens, 3. output cylindrical lens, 4. electrode probes, and 5. chuck for holding sample.

Fig. 11 Image of deflected beam on a screen for applied voltages of ± 300 and 0 V.

of the device, and it can easily work as a 1×2 optical switch.

6 Conclusion

We have successfully fabricated and demonstrated an EO polymer-based waveguide beam deflector. The improved EO polymer has long term thermal stability, which provides for the development of a commercial device. The thin-film waveguide beam deflector device is demonstrated using an EO polymer waveguide and prism array. The waveguide is fabricated with an electrode structure defining the prism cascade within the planar waveguide. The deflection efficiency of 28 mrad/kV and the maximum deflection angle of ±8.4 mrad at ±300 V is obtained for this first demonstration device. Further optimization of poling and processing is likely to improve these results by at least an order of magnitude.

References

1. M. Shimizu, K. Yoshida, and R. Ohta, ''Mechanical optical switch for single-mode fiber,'' *IEICE Trans. Commun.* **E76-B**(4), 370–374 (April 1998).
2. C. Gonzalez and S. D. Collins, ''Micromachined $1\times n$ fiber-optic switch,'' *IEEE Photonics Technol. Lett.* **9**(5), 616–618 (1997).
3. J. E. Ford and D. J. DiGiovanni, ''$1\times N$ fiber bundle scanning switch,'' *IEEE Photonics Technol. Lett.* **10**(7), 967–969 (July 1998).
4. D. Kip, M. Wesner, E. Kratzig, V. Shandarov, and P. Moretti, ''All-optical beam deflection and switching in strontium-barium-niobate waveguides,'' *Appl. Phys. Lett.* **72**(16), 1960–1962 (20 April 1998).
5. M. D. Himel, X. Shi, X. Q. Hu, M. G. Moharam, and K. H. Guenther, ''Electrooptic beam deflection using the leaky mode of a planar waveguide,'' *IEEE Photonics Technol. Lett.* **3**, 921–923 (1991).
6. Y. Shi, W. Wang, J. H. Bechtel, A. Chen, S. Garner, S. Kalluri, W. H. Steier, D. Chen, H. R. Fetterman, L. R. Dalton, and L. Yu, ''Fabrication and characterization of high-speed polyurethane-disperse red 19 integrated electrooptic modulators for analog system applications,'' *IEEE J. Sel. Top. Quantum Electron.* **2**(2), 289–299 (1996).
7. S. Lee, S. M. Garner, V. Chuyanov, H. Zhang, W. H. Steier, F. Wang, L. R. Dalton, A. Udupa, and H. R. Fetterman, ''Optical intensity modulator based on a novel electrooptic polymer incorporating high mu beta chromophore,'' *IEEE J. Quantum Electron.* **36**(5), 527–532 (May 2000).
8. W. Sotoyama, S. Tatsuura, and T. Yoshimura, ''Electro-optic side-chain polyimide system with large optical nonlinearity and high thermal stability,'' *Appl. Phys. Lett.* **64**(17), 2197–2199 (25 April 1994).
9. L. Sun, J. Maki, J. Taboada, D. An, Z. Han, X. Lu, R. Chen, and S. Tang, ''Laser beam deflector based on a domain-inverted electrooptic polymeric waveguide prism array,'' *Proc. SPIE* **3632**, 134–141 (1999).
10. A. Yariv, *Quantum Electronics*, 3rd ed., pp. 323, John Wiley & Sons, New York (1989).
11. C. Zhang, C. Wang, L. R. Dalton, G. Sun, H. Zhang, and W. H. Steier, ''Investigation on new polyurethanes and incorporation of a soluble high $\mu\beta$ chromophore for electro-optic applications,'' *American Chemistry Society Symposium* **40**(1), 51–52 (March 1999).
12. Y. Chiu, D. Stancil, T. Schlesinger, and W. Risk, ''Electro-optic beam scanner in KTiOPO$_4$'' *Appl. Phys. Lett.* **69**(21), 3134–3136 (18 November 1996).
13. K. Gahagan, V. Gopalan, J. Robinson, Q. Jia, T. Mitchell, M. Kawas, T. Schlesinger, and D. Stancil, ''Integrated electro-optic lens/scanner in a LiTaO$_3$ single crystal,'' *Appl. Opt.* **38**(7/1), 1186–1190 (March 1999).

Lin Sun is a fabrication engineer at Radiant Photonics, Inc. She received her BS degree in chemistry with Honors from The University of Xinjiang, China, in 1986. She received her MS in chemistry in 1989 from Shanghai Institute of Organic Chemistry, Academy of Sciences, in China. In 2000, she received her MS in optoelectronics at the University of Texas at Austin.

Dechang An is a PhD candidate working on polymer-based electro-optic devices at the Microelectronics Research Center at the University of Texas at Austin. He received his BS and MS in optics from Shandong University and the Institute of Physics, Chinese Academy of Sciences, in 1983 and 1990, respectively.

Jeffery J. Maki is Director of Switch Products at Radiant Photonics, Inc. He received his BS degree in mathematics and physics with Honors in 1984 from Lewis and Clark College, Portland, Oregon, and his PhD in optics in 1992 from The Institute of Optics, University of Rochester, New York. His graduate work was in nonlinear and quantum optics. In 1992, he took a postdoctoral position with the Department of Physics, Oregon State University, Corvallis, where he worked on frequency-control techniques of semiconductor lasers for atom trapping, and helped develop an atomic funnel for matter-wave interferometry. In 1994, as a visiting scholar, he joined the Laboratory for Chemical and Biological Dynamics, Department of Chemistry, University of Leuven, Belgium, where he conducted research on the nonlinear-optical properties of chiral-polymer thin films. He has been with Radiant Photonics (formerly Radiant Research) since 1996. He is a member of OSA, SPIE, IEEE, and Phi Kappa Phi.

Cheng Zhang received his PhD in organic and polymer chemistry from the Department of Chemistry, University of Southern California (USC), in 1999. He is now the research associate and the leader of Prof. Larry R. Dalton's polymeric electro-optic material research group at USC. He specializes in molecular design and multistep synthesis of state-of-the-art second-order nonlinear optical chromophores and NLO polymers including polymethacrylates, polyurethanes, polyester, polycarbonates and polyepoxides, polyimides, polyethers, and fluorinated polymers. He is the principal inventor of the CLD series of NLO chromophores, which are used in the fabrication of practical EO devices.

Larry R. Dalton holds the positions of Distinguished Professor of Chemistry and Engineering at the University of Washington (since 1998) and the University of Southern California (since 1981). He also directs and codirects scientific centers and institutes at the two universities, including the Loker Hydrocarbon Research Institute (since 1994). He was awarded BS and MS degrees in chemistry from the Honors College of Michigan State University with high-

est honors in 1965 and 1966. He received AM and PhD degrees in chemistry from Harvard University in 1971. Awards include the 2000 Distinguished Alumni Award of Michigan State University, the 1997 Richard C. Tolman Metal of the American Chemical Society, the 1996 Paul C. Cross Lectureship of the University of Washington, the 1995 NASA Lectureship, 54th Frontiers in Chemistry Lecture Series

of Case Western Reserve University, the 1986 Burlington Northern Foundation Faculty Achievement Award, an NIH Research Career Development Award (1976), a Camille and Henry Dreyfus Teacher-Scholar Award (1975), and an Alfred P. Sloan Fellowship (1974). He is the author of more than 400 publications and patents.